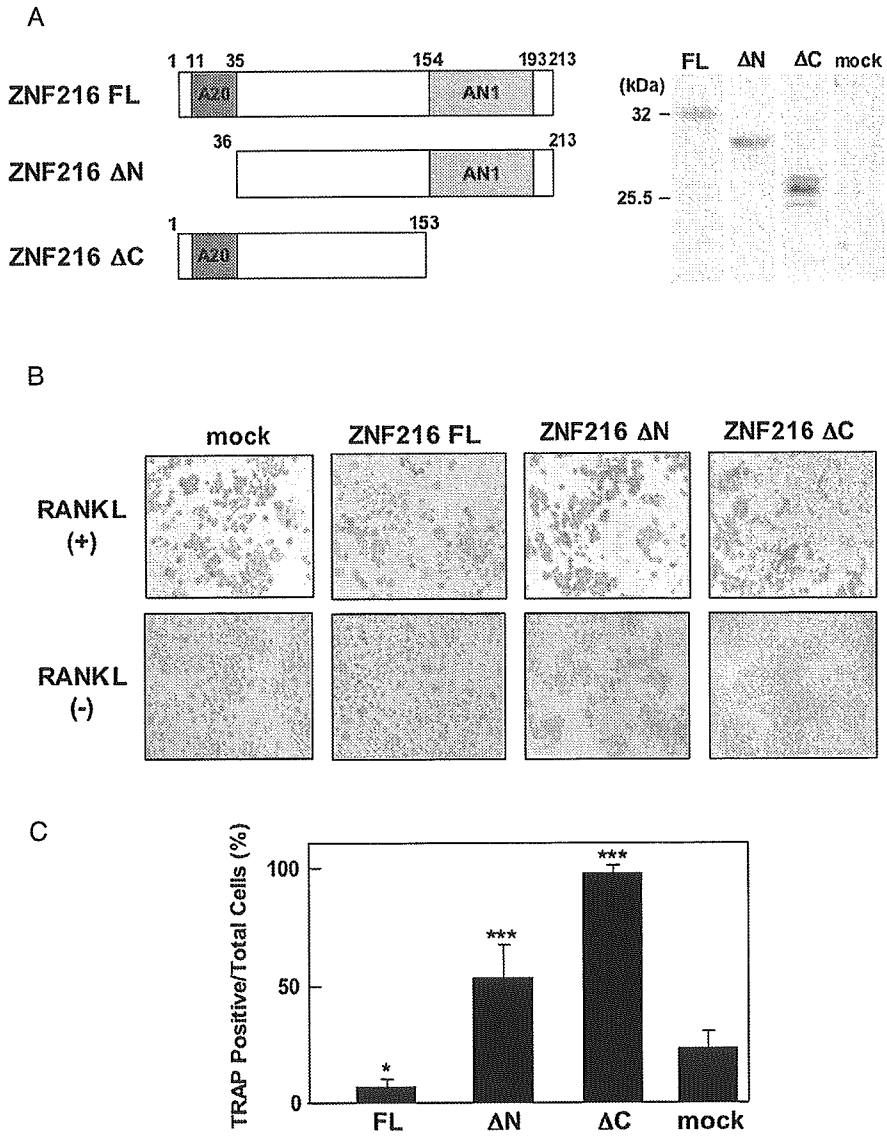

Figure 2: ZNF216 inhibits osteoclastogenesis. (A) Schematic presentation of ZNF216 and its deletion mutants (left panel). Full-length ZNF216 (213 amino acids) is denoted as ZNF216-FL. A20-like (*dark gray box*) or AN1-like (*gray box*) zinc finger domains were deleted in ZNF216-ΔN or ZNF216-ΔC, respectively. The number represents the positions of the deleted amino acid residues. Expression of ZNF216 and its mutants in RAW264.7 cells (right panel). The expression levels of the proteins in stable transfectants were comparable. ZNF216 proteins were detected by immunoblotting with anti-FLAG antibody. (B) Ectopic expression of ZNF216 inhibits RANKL-mediated osteoclastogenesis in RAW264.7 cells. Three individual RAW264.7 cell clones stably expressing full-length or truncated forms of the zinc finger domains were seeded and treated with (upper panels) or without (lower panels) RANKL (10 ng/mL). After 48 hr, cells were fixed and TRAP activity was determined. No TRAP-positive cells were observed in all cell lines without RANKL treatment. (C) The number of TRAP-positive (purple) cells, in (B), were quantified. Results represent the average values from the three clones. $^{*}P < 0.05$ vs. mock-infected cells; $^{***}P < 0.005$ vs. mock-infected cells.

ZNF216 in the NF-κB Signaling Pathway

The inhibitory effects of ZNF216 we observed, along with a recent report indicating that ZNF216 inhibits NF-κB activation (29), prompted us to investigate the relationship between ZNF216 and NF-κB signaling in osteoclastogenesis. For NF-κB activation, the degradation of its inhibitory binding molecule, IκB, is crucial. Activation of the NF-κB pathway requires phosphorylation of IκB leading to its degradation via the ubiquitin-proteasome system (30). As shown in Figure 3A, IκBα was rapidly degraded by LPS in mock-transfected RAW264.7 cells. Neither the full-length nor the truncated mutants of ZNF216 affected IκBα degradation (Fig. 3A). NF-κB dissociated from IκB exposes its nuclear localization signal. Thus, we investigated cytoplasmic to nuclear translocation of NF-κB in RANK293 cells, which are a cell line derived from HEK293 cell stably transfected with a vector to express RANK. Cells were treated with RANKL, and the nuclear fraction subsequently extracted and monitored for the translocation of NF-κB. As shown in Figure 3B, there were no significant alterations in the nuclear translocation of p50, p52, and p60 NF-κB subunits between mock- and ZNF216-infected cells. ZNF216 was localized predominantly in the cytoplasm and to a lesser extent in the nucleus (data not shown). We next examined whether ectopic expression of ZNF216 disrupted the binding ability of NF-κB to its target promoter. Although no band shift was observed in nuclear extracts from nontreated RANK293 cells, RANKL-treated cell extracts showed a prominent band shift (Fig. 3C). The binding ability of NF-κB to oligo probe was not affected by expression of either full-length or truncated mutants of ZNF216 (Fig. 3C). Finally, neither the expression of full-length nor truncated mutants of ZNF216 affected transcription of the reporter luciferase gene driven by the NF-κB promoter after TNFα stimulation (Fig. 3D) or the AP-1 promoter (Fig. 3E). Together, these results suggest that ZNF216 is not directly involved in the NF-κB signaling pathway.

DISCUSSION

In the present study, we have identified genes regulated in RANKL-induced osteoclast differentiation. Although some of the up-regulated genes have been previously reported to be involved in osteoclast differentiation, the majority of the down-regulated genes have not been described. Recently, it was demonstrated that the ITAM-bearing protein family of transmembrane adaptors, such as DAP12, play critical roles in osteoclast development and function (31–33). These co-stimulatory adaptors are known to be associated with Fc receptors in the modulation of their signals (34,35). Notably, the expression of Fc receptors were down-regulated during osteoclast differentiation in our study (Table 2), suggesting that the function of the ITAMs may not associated with the Fc receptors, but other cell surface molecules, such as TREM2 (36,37).

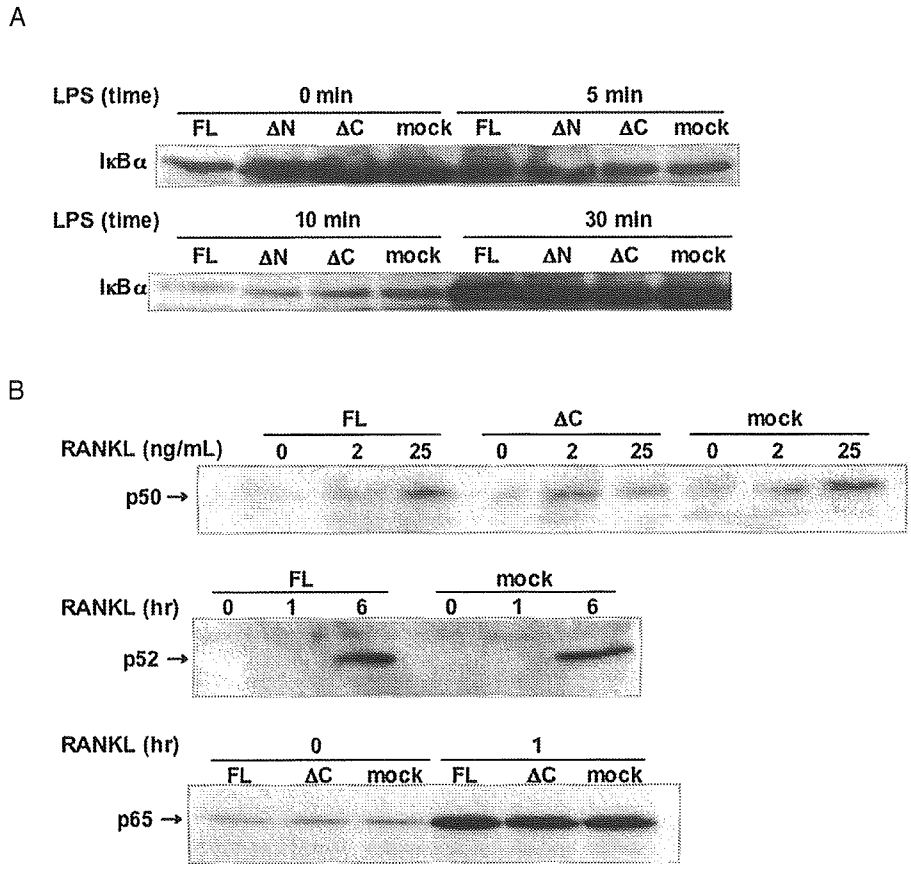

Figure 3: ZNF216 does not inhibit the NF-κB pathway. (A) Degradation of IκBα protein by LPS. RAW264.7 cells stably expressing the indicated constructs were stimulated with 10 μg/mL LPS. At the indicated time points, cells were lysed and analyzed for IκBα protein by immunoblotting. (B) Expression levels of the NF-κB protein subunits. RANK293 cells were transfected with the indicated vector constructs. Cells were then treated with 0, 2, and 25 ng/mL RANKL for 30 min. Nuclear fraction was isolated and subjected to immunoblot analysis for the p50, p52, and p65 NF-κB subunits. Cells were treated with 10 ng/mL RANKL for the indicated time periods, and immunoblot analyses were performed. (C) RANKL-dependent band shift of NF-κB. EMSA analyses were conducted with nuclear extracts from the indicated vector constructs in RANK293 cells as described in Materials and Methods. Arrow indicates nonbound free probe. (D) TNFα-dependent NF-κB reporter gene activation. HEK293 cells were transfected with 5 ng or 25 ng of the indicated ZNF216 constructs and 10 ng of pNF-κB-Luc. All luciferase activities were corrected with renilla luciferase activities. Each experiment was performed at least in triplicate, and data are expressed as the means ± SD. (E) Effect on AP-1-dependent transcription. HEK293 cells were transfected with 10 ng MEKK-expressing plasmid and 250 ng ZNF216 full-length plasmid. All luciferase activities were corrected with renilla luciferase activities. Each experiment was performed at least in duplicate, and data are expressed as the means ± SD. *(Continued)*

Interferons have also been shown to play important roles in physiological and pathological osteoclast function (38). IFNβ is induced by the RANKL-RANK pathway through Fos and inhibits the function of the transcription factor, forming a negative feedback loop (39). In our studies, significant decreases in

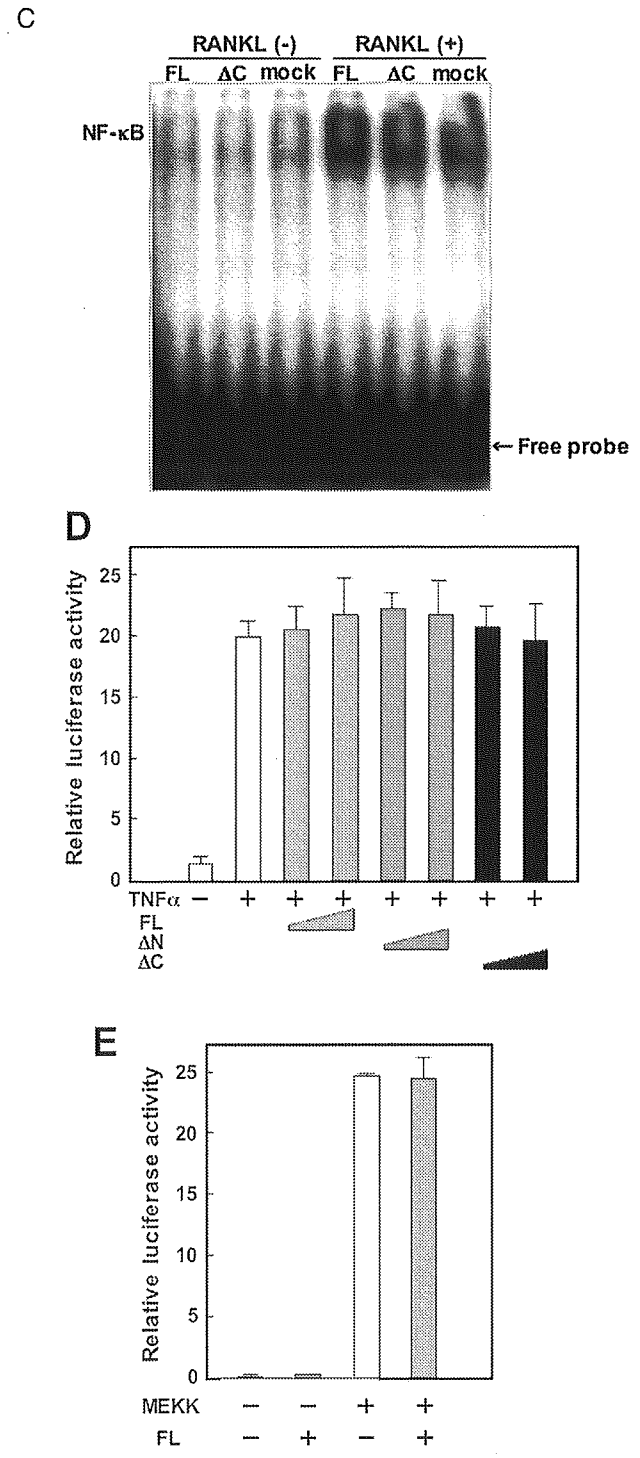

Figure 3: (Continued)

the expression of a series of IFN-responsive genes were observed at the later stages (48 hr) of differentiation. We speculate that the feedback loop may regulate the early phase of differentiation and that, once the cells pass through that phase, they may become resistant to IFN in terms of the osteoclastogenesis. In support, fos has been shown to be replaced by known downstream effectors, including Fra1 and Fra2 (Table 2) in the later phase of osteoclast differentiation (40). The regulation and relationship between IFN and fos family proteins are interesting issues worth further study.

In addition, several genes for lysosomal enzymes and the lysosomal marker, LAMP2, were shown to be down-regulated. Active osteoclasts are highly polarized and possess bone-resorbing activity by providing acidified compartments and hydrolyzing enzymes, including MMP9 and cathepsin K, between the apical surface and sealing zones of osteoclasts and the bone surface. It has been reported that the resorption compartment is similar to early endosomes and lysosomes (41,42). The decrease in the expression of the lysosomal genes throughout osteoclast differentiation that were shown in our study may support the idea that the ruffled border membrane and the acidified extracellular compartment are specialized for bone matrix resorption and different from the lysosomes observed in other cell types.

We also identify a gene encoding ZNF216 as up-regulated by RANKL-induced osteoclast differentiation. Furthermore, ectopic expression of full-length ZNF216 inhibited but the zinc finger-truncated mutants accelerated osteoclast differentiation. Because the gene was also up-regulated by TNFα, RANKL may share common machinery with TNFα in induction of ZNF216 expression. Factors known to activate NF-κB, such as LPS and TPA, also up-regulated the expression of ZNF216. It is of interest that the promoter region of human ZNF216 gene contains a possible NF-κB response element (data not shown). These results suggested that a probable factor involved in the induction of ZNF216 is the NF-κB transcription factor, although further experiments are required. In support, IFNβ is a strong negative regulator of osteoclastogenesis (43,44), and expression of ZNF216 suppressed osteoclast differentiation in our study. Therefore, ZNF216 may take part in the IFN-mediated regulatory mechanism NF-κB.

The precise molecular function of ZNF216 is still unclear. It has been reported that ZNF216 may inhibit the NF-κB pathway (29). Although we have examined the influence of ZNF216 on NF-κB activation, neither inhibition of nuclear translocation nor DNA-binding ability of NF-κB was reproduced by ectopic expression of full-length or truncated mutants of ZNF216 (not shown). Furthermore, we have tested the NF-κB inhibitory activity of ZNF216, as well as A20 protein, using reporter gene constructs. Ectopic expression of A20, but not full-length ZNF216, strongly inhibited NF-κB activation (data not shown). In addition, no endogenous NEMO or RIP protein was detected in a proteome analysis of the ZNF216 complex (unpublished observation). Therefore, ZNF216

does not seem to be a direct regulator of the NF-κB signaling pathway, although its involvement is still under investigation. It was recently described that one of the seven A20-type zinc finger domains in A20 protein possesses E3 ubiquitin ligase activity (45). Thus, ZNF216 also may be involved in ubiquitin-related systems. It is of interest that our expression studies resulted in opposing phenotypes in osteoclastogenesis that were largely dependent on the mutation. Thus, the truncated mutants may act in a dominant negative manner compared with the endogenous or wild-type ZNF216. How does ZNF216 inhibit osteoclastogenesis without affecting NF-κB pathway? Future studies will be aimed at elucidation of the molecular mechanisms involved in ZNF216-mediated osteoclast differentiation.

ACKNOWLEDGMENT

The authors dedicate this paper to our colleague, Dr. Katsunori Mizuno, who passed in December 2004. We are grateful to Drs. Kunihiro Matsumoto and Naoki Sakurai for providing RANK293 cells; Dr. Koichi Matsuo for helpful discussions; and John Grzesiak for proofreading the manuscript. This work is supported in part by a grant from the Program for Promotion of Fundamental Studies in Health Sciences of the Organization for Pharmaceutical Safety and Research of Japan, and by a Research Grant for Longevity Sciences from the Ministry of Health, Labor and Welfare.

REFERENCES

1. Ash P, Loutit JF, Townsend KM. Osteoclasts derived from haematopoietic stem cells. Nature **1980**, *283*, 669–670.

2. Suda T, Udagawa N, Takahashi N. Osteoclast generation. In: (Bilezikian JP, Raisz LG, Rodan CA, Eds. *Principles of Bone Biology*. San Diego: Academic Press, 1996, 87–102.

3. Roodman GD. Advances in bone biology: The osteoclast. Endocr Rev **1996**, 17; 308–332.

4. Yoshida H, Hayashi S, Kunisada T, Ogawa M, Nishikawa S, Okamura H, Sudo T, Shultz LD, Nishikawa S. The murine mutation osteopetrosis is in the coding region of the macrophage colony stimulating factor gene Nature **1990**, *345*, 442–444.

5. Pfeilschifter J, Chenu C, Bird A, Mundy GR, Roodman GD. Interleukin-1 and tumor necrosis factor stimulate the formation of human osteoclast-like cells in vitro. J Bone Miner Res **1989**, *4*, 113–118.

6. Kobayashi K, Takahashi N, Jimi E, Udagawa N, Takami M, Kotake S, Nakagawa N, Kinosaki M, Yamaguchi K, Shima N, Yasuda H, Morinaga T, Higashio K, Martin TJ, Suda T. Tumor necrosis factor alpha stimulates osteoclast differentiation by a mechanism independent of the ODF/RANKL-RANK interaction. J Exp Med **2000**, *191*, 275–286.

7. Lacey DL, Timms E, Tan H-L, Kelley MJ, Dunstan CR, Burgess T, Elliott R, Colombero A, Elliott G, Scully S, Hsu H, Sullivan J, Hawkins N, Davy E, Capparelli C, Eli A, Qian Y-X, Kaufman S, Sarosi I, Shalhoub V, Senaldi G, Guo J, Delaney J, Boyle

WJ. Osteoprotegerin ligand is a cytokine that regulates osteoclast differentiation and activation. Cell **1998**, *93*, 165–176

8. Yasuda H, Shima N, Nakagawa N, Yamaguchi K, Kinosaki M, Mochizuki S, Tomoyasu A, Yano K, Goto M, Murakami A, Tsuda E, Morinaga T, Higashio K, Udagawa N, Takahashi N, Suda T. Osteoclast differentiation factor is a ligand for osteoprotegerin/osteoclastogenesis-inhibitory factor and is identical to TRANCE/RANKL. Proc Natl Acad Sci USA **1998**, *95*, 3597–3602.

9. Kong Y-Y, Yoshida H, Sarosi I, Tan H-L, Timms E, Capparelli C, Morony S, Oliveira-dos-Santos AJ, Van G, Itie A, Khoo W, Wakeham A, Dunstan CR, Lacey DL, Mak TW, Boyle WJ, Penninger JM. OPGL is a key regulator of osteoclastogenesis, lymphocyte development and lymph-node organogenesis. Nature **1999**, *397*, 315–323

10. Li J, Sarosi I, Yan X-Q, Morony S, Capparelli C, Tan H-L, McCabe S, Elliott R, Scully S, Van G, Kaufman S, Juan S-C, Sun Y, Tarpley J, Martin L, Christensen K, McCabe J, Kostenuik P, Hsu H, Fletcher F, Dunstan CR, Lacey DL, Boyle WJ. RANK is the intrinsic hematopoietic cell surface receptor that controls osteoclastogenesis and regulation of bone mass and calcium metabolism. Proc Natl Acad Sci USA **2000**, *97*, 1566–1571.

11. Fuller K, Wong B, Fox S, Choi Y, Chambers TJ. TRANCE is necessary and sufficient for osteoblast-mediated activation of bone resorption in osteoclasts. J Exp Med **1998**, *188*, 997–1001.

12. Lotsova V, Caamano J, Loy J, Yang Y, Lewin A, Bravo R. Osteopetrosis in mice lacking NF-κB1 and NF-κB2. Nat Med **1997**, *3*, 1285–1289.

13. Grigoriadis AE, Wang ZQ, Cecchini MG, Hofstetter W, Felix R, Fleisch HA, Wagner EF. c-Fos: A key regulator of osteoclast-macrophage lineage determination and bone remodeling. Science **1994**, *266*, 443–448.

14. Wagner EF, Matsuo K. Signalling in osteoclasts and the role of Fos/AP1 proteins. Ann Rheum Dis **2003**, *62*, 83–85.

15. Soriano P, Montgomery C, Geske R, Bradley A. Targeted disruption of the c-src proto-oncogene leads to osteopetrosis in mice. Cell **1991**, *64*, 693–702.

16. Boyce BF, Yoneda T, Lowe C, Soriano P, Mundy GR. Requirement of pp60c-src expression for osteoclasts to form ruffled borders and resorb bone in mice. J Clin Invest **1992**, *90*, 1622–1627.

17. Tanaka S, Takahashi N, Udagawa N, Sasaki T, Fukui Y, Kurokawa T, Suda T. Osteoclasts express high levels of p60c-src, preferentially on ruffled border membranes. FEBS Lett **1992**, *313*, 85–89.

18. Mizukami J, Takaesu G, Akatsuka H, Sakurai H, Ninomiya-Tsuji J, Matsumoto K, Sakurai N. Receptor activator of NF-kappaB ligand (RANKL) activates TAK1 mitogen-activated protein kinase kinase kinase through a signaling complex containing RANK, TAB2, and TRAF6. Mol Cell Biol **2002**, *22*, 992–1000.

19. Yousef, AA. IL-4 abrogates osteoclastogenesis through STAT6-dependent inhibition of NF-κ B J Clin Invest **2001**, *107*, 1375–1385.

20. Battaglino R, Kim D, Fu J, Vaage B, Fu XY, Stashenko P. c-myc is required for osteoclast differentiation. J Bone Miner Res **2002**, *17*, 763–773.

21. Matsuo K, Galson DL, Zhao C, Peng L, Laplace C, Wang KZ, Bachler MA, Amano H, Aburatani H, Ishikawa H, Wagner EF. Nuclear factor of activated T-cells (NFAT) rescues osteoclastogenesis in precursors lacking c-Fos. J Biol Chem **2004**, *279*, 26475–26480.

22. Takayanagi H, Ogasawara K, Hida S, Chiba T, Murata S, Sato K, Takaoka A, Yokochi T, Oda H, Tanaka K, Nakamura K, Taniguchi T. T-cell-mediated regulation of

osteoclastogenesis by signalling cross-talk between RANKL and IFNγ. Nature **2000**, *408*, 600–605.

23. Scott DA, Greinwald JH, Jr, Marietta JR, Drury S, Swiderski RE, Vinas A, DeAngelis MM, Carmi R, Ramesh A, Kraft ML, Elbedour K, Skworak AB, Friedman RA, Srikumari Srisailapathy CR, Verhoeven K, Van Gamp G, Lovett M, Deininger PL, Batzer MA, Morton CC, Keats BJ, Smith RJ, Sheffield VC. Identification and mutation analysis of a cochlear-expressed, zinc finger protein gene at the DFNB7/11 and dn hearing-loss loci on human chromosome 9q and mouse chromosome 19. Gene **1998** *215*, 461–469.

24. Hofbauer LC, Khosla S, Dunstan CR, Lacey DL, Boyle WJ, Riggs BL. The roles of osteoprotegerin and osteoprotegerin ligand in the paracrine regulation of bone resorption. J Bone Miner Res **2000**, *15*, 2–12.

25. Castagna M, Takai Y, Kaibuchi K, Sano K, Kikkawa U, Nishizuka Y. Direct activation of calcium-activated, phospholipid-dependent protein kinase by tumor-promoting phorbol esters. J Biol Chem, **1982** *257*, 7847–7851.

26. Hirano M, Hirai S, Mizuno K, Osada S, Hosaka M, Ohno S. A protein kinase C isoenzyme, nPKCε, is involved in the activation of NF-κB by 12-O-tetradecanoylphorbol-13-acetate (TPA) in rat 3Y1 fibroblasts. Biochem Biophys Res Commun **1995**, *206*, 429–436.

27. Chen Y, Wu Q, Song S-Y, Su W-J. Activation of JNK by TPA promotes apoptosis via PKC pathway in gastric cancer cells. World J. Gastroenterol **2002**, *8*, 1014–1018.

28. Linnen JM, Bailey CP, Weeks D. L. Two related localized mRNAs from Xenopus laevis encode ubiquitin-like fusion proteins. Gene **1993**, *128*, 181–188

29. Huang J, Teng L, Li L, Liu T, Li L, Chen D, Xu LG, Zhai Z, Shu HB. ZNF216 is an A20-like and IκB kinase γ-interacting inhibitor of NFκB activation. J Biol Chem **2004**, *279*, 16847–16853.

30. Whiteside ST, Israel A. IκB proteins: Structure, function and regulation. Semin Cancer Biol **1997**, *8*, 75–82.

31. Kaifu T, Nakahara J, Inui M, Mishima K, Momiyama T, Kaji M, Sugahara A, Koito H, Ujike-Asai A, Nakamura A, Kanazawa K, Tan-Takeuchi K, Iwasaki K, Yokoyama WM, Kudo A, Fujiwara M, Asou H, Takai T. Osteopetrosis and thalamic hypomyelinosis with synaptic degeneration in DAP12-deficient mice. J Clin Invest **2003**, *111*, 323–332.

32. Koga T, Inui M, Inoue K, Kim S, Suematsu A, Kobayashi E, Iwata T, Ohnishi H, Matozaki T, Kodama T, Taniguchi T, Takayanagi H, Takai T. Costimulatory signals mediated by the ITAM motif cooperate with RANKL for bone homeostasis. Nature **2004**, *428*, 758–763.

33. Mocsai A, Humphrey MB, Van Ziffle JA, Hu Y, Burghardt A, Spusta SC, Majumdar S, Lanier LL, Lowell CA, Nakamura MC. The immunomodulatory adapter proteins DAP12 and Fc receptor gamma-chain (FcRgamma) regulate development of functional osteoclasts through the Syk tyrosine kinase. Proc Natl Acad Sci USA **2004**, *101*, 6158–6163.

34. Daeron M. Fc receptor biology. Annu Rev Immunol **1997**, *15*, 203–234.

35. Nakajima H, Samaridis J, Angman L, Colonna M. Human myeloid cells express an activating ILT receptor (ILT1) that associates with Fc receptor gamma-chain. J Immunol **1999**, *162*, 5–8.

36. Cella M, Buonsanti C, Strader C, Kondo T, Salmaggi A, Colonna M. Impaired differentiation of osteoclasts in TREM-2-deficient individuals. J Exp Med **2003**, *198*, 645–651.

37. Paloneva J, Mandelin J, Kiialainen A, Bohling T, Prudlo J, Hakola P, Haltia M, Konttinen YT, Peltonen L. DAP12/TREM2 deficiency results in impaired osteoclast differentiation and osteoporotic features. J Exp Med **2003**, *198*, 669–675.

38. Takayanagi H, Kim S, Taniguchi T. Signaling crosstalk between RANKL and interferons in osteoclast differentiation. Arthritis Res **2002a**, *4*, S227–S232.

39. Takayanagi H, Kim S, Matsuo K, Suzuki H, Suzuki T, Sato K, Yokochi T, Oda H, Nakamura K, Ida N, Wagner EF, Taniguchi T. RANKL maintains bone homeostasis through c-Fos-dependent induction of interferon-beta. Nature **2002b**, *416*, 744–749.

40. Matsuo K, Owens JM, Tonko M, Elliott C, Chambers TJ, Wagner EF. Fosl1 is a transcriptional target of c-Fos during osteoclast differentiation Nat Genet **2000**, *24*, 184–187.

41. Palokangas H, Mulari M, Vaananen HK. Endocytic pathway from the basal plasma membrane to the ruffled border membrane in bone-resorbing osteoclasts. J Cell Sci **1997**, *110*, 1767–1780.

42. Stenbeck G. Formation and function of the ruffled border in osteoclasts. Semin Cell Dev Biol **2002**, *13*, 285–292.

43. Gowen M, Mundy GR. Actions of recombinant interleukin 1, interleukin 2, and interferon-gamma on bone resorption in vitro. J Immunol **1986**, *136*, 2478–2482.

44. Takahashi N, Mundy GR, Roodman GD. Recombinant human interferon-gamma inhibits formation of human osteoclast-like cells. J Immunol **1986**, *137*, 3544–3549.

45. Wertz IE, O'Rourke KM, Zhou H, Eby M, Aravind L, Seshagiri S, Wu P, Wiesmann C, Baker R, Boone DL, Ma A, Koonin EV, Dixit VM. De-ubiquitination and ubiquitin ligase domains of A20 downregulate NF-kappaB signalling. **2004**, *430*, 694–699.

Available online at www.sciencedirect.com
SCIENCE DIRECT®
Archives of Biochemistry and Biophysics 435 (2005) 42–49
ABB
www.elsevier.com/locate/yabbi

Detection of S-glutathionylated proteins by glutathione *S*-transferase overlay

Guang Cheng[a], Yoshitaka Ikeda[b], Yoshihito Iuchi[a], Junichi Fujii[a,*]

[a] *Department of Biomolecular Function, Yamagata University Graduate School of Medicine, 2-2-2 Iidanishi, Yamagata 990-9585, Japan*
[b] *Division of Molecular Cell Biology, Department of Biomolecular Sciences, Saga University Faculty of Medicine, 5-1-1 Nabeshima, Saga 849-8501, Japan*

Received 13 September 2004, and in revised form 25 November 2004
Available online 4 January 2005

Abstract

Oxidative and nitrosative stress lead to the S-glutathionylation of proteins and subsequent functional impairment. Glutathione *S*-transferase (GST) from *Schistosoma japonicum* was found to bind to the glutathione moiety of S-glutathionylated proteins, thus establishing a convenient method for detecting S-glutathionylated proteins by biotinylated GST. Applications of this method to proteins that were prepared from cultured cells and blotted onto a membrane exhibited numerous positive bands, which were abolished by treatment with dithiothreitol. Treatment of a cellular extract with nitrosoglutathione led to enhanced staining of the bands in a dose-dependent manner. The method was also applicable for the histochemical detection of S-glutathionylated proteins in situ. The positive staining by biotin–GST became faint in the presence of S-glutathionylated ovalbumin, suggesting that the reaction is specific to S-glutathionylated proteins. Collectively, these data indicate that the method established here is simple and useful for detecting S-glutathionylated proteins on blotted membrane and in situ.

Keywords: Glutathione; S-Glutathionylation; Glutathione *S*-transferase; Nitrosoglutathione; Reactive oxygen species; Reactive nitrogen oxide species

Various types of stress increase the production of reactive oxygen species (ROS)[1] and reactive nitrogen oxide species (RNOS), which, in turn, cause the oxidative modification of biological compounds [1]. The sulfhydryl group is the most susceptible group in proteins to ROS and RNOS. When an essential sulfhydryl group in proteins is modified, the cells become dysfunctional. While ROS converts sulfhydryl groups to sulfenic, sulfinic, and sulfonic acid derivatives, the groups are also oxidized to form disulfides by reacting with other thiols. The formation of intra- and inter-molecular disulfide bonds, as a response to oxidative and nitrosative stress, is common [2]. The DNA binding activity of oxidative stress-sensitive transcription factors, such as c-Jun [3] and Nrf2 [4], is directly or indirectly regulated by ROS/RNOS.

Glutathione, an abundant tripeptide, contains a sulfhydryl group and is involved in maintaining redox balance in cells. An accumulating body of evidence

* Corresponding author. Present address. Department of Biomolecular Function, Yamagata University Graduate School of Medicine, 2-2-2 Iidanishi, Yamagata 990-9585, Japan. Fax: +81 23 628 5230.
E-mail address: jfujii@med.id.yamagata-u.ac.jp (J. Fujii).

[1] *Abbreviations used:* ROS, reactive oxygen species; RNOS, reactive nitrogen oxide species; GSH, reduced from of glutathione; GSSG, oxidized form of glutathione; GST, glutathione *S*-transferase (*Schistosoma japonicum* origin); CDNB, 1-chloro-2,4-dinitrobenzene; GSNO, *S*-nitrosoglutathione; BSA, bovine serum albumin; OVA, ovalbumin; PBS, phosphate-buffered saline; DTT, dithiothreitol; HRP, horseradish peroxidase; SNAP, *S*-nitroso-*N*-acetyl-D,L-penicillamine; DMEM, Dulbecco's modified minimum essential medium; FBS, fetal bovine serum; BSO, buthionine sulfoximine; BCNU, 1,3-bis[2-chlorethyl]-1-nitrosourea; NAC, *N*-acetylcysteine.

0003-9861/$ - see front matter © 2005 Elsevier Inc. All rights reserved.
doi:10.1016/j.abb.2004.12.016

indicates that an increase in mixed disulfide formation between glutathione and protein thiols occurs during oxidative and nitrosative stress [5–7]. When S-glutathionylation occurs at an essential sulfhydryl group, this also affects protein function [6]. For example, the function of glyceraldehyde-3-phosphate dehydrogenase [8], aldose reductase [9], annexin A2 [10], protein kinase C [11], carbonic anhydrase III [12], and tubulin [13] are all known to be affected by S-glutathionylation. On the other hand, the antioxidative protein, peroxiredoxin 6, is activated as the result of this modification [14]. Thus, S-glutathionylation is not only a marker for oxidative stress, but also is actually involved in the regulation of cellular function [6]. The S-glutathionylation reaction is partially reversed by glutaredoxin, which releases glutathione moiety from the modified protein in conjunction with the formation of glutathione disulfide [15–17].

A number of S-glutathionylated proteins have been identified. Several attempts have been made to detect S-glutathionylated proteins by a proteomic approach. The most popular method is the use of a radioisotope, ^{35}S, which labels the sulfur atom of a glutathione moiety in S-glutathionylated proteins. Using this technique, several S-glutathionlyated proteins have been identified [18,19]. However, this is applicable only for in vitro experiments and such labeling may cause experimental artifacts, due to metabolic labeling [20]. A biotinylated membrane-permeable analogue of glutathione was developed to detect proteins that are susceptible to specific stimuli including *S*-nitrosoglutathione (GSNO). Annexin II was identified as a reactive protein by this method [21]. The specific reduction of the mixed disulfides by glutaredoxin followed by reaction with *N*-ethylmaleimide–biotin led to the detection of S-glutathionylated proteins [22]. Using this method, 43 different proteins were found to be S-glutathionylated. A method using GSNO–Sepharose was also developed to detect proteins that form GSNO-induced mixed disulfides [6]. These methods are sophisticated, but rather complex, and, hence, applicable for the analysis of small numbers of samples. An antibody against glutathione has been raised, but its use has been applied for limited so far [23–26]. The development of a simple and widely applicable method for detecting S-glutathionylated proteins is still awaited.

In this study, we found that glutathione *S*-transferase (GST) from *Schistosoma japonicum* binds the glutathione moiety of S-glutathionylated proteins and thus represents a simple method, employing biotinylated GST, for detecting S-glutathionylated proteins. Since this method uses GST as a glutathione-detecting probe, similar to an antibody, it can be performed in a manner analogous to an immunoblot analysis. In addition, it is also applicable for the histochemical detection of S-glutathionylated proteins in situ.

Materials and methods

Materials

Glutathione, reduced and oxidized forms, was purchased from Roche (Mannheim, Germany). 1-Chloro-2,4-dinitrobenzene (CDNB), 4-chloro-1-naphthol, GSNO, and isopropyl β-D-thiogalactoside (IPTG) were from Wako Pure Chemicals (Osaka, Japan). *N*-Hydroxysuccinimide (NHS)–biotin and horseradish peroxidase (HRP)-conjugated streptavidin were obtained from Pierce (Rockford, IL). Diamide was from ICN (Aurora, OH). Glutathione–Sepharose 4B and PD-10 were from Pharmacia (Wilksröms, Sweden). All other reagents used were of the highest quality available. Experiments using animals were performed in accordance with the declaration of Helsinki under the protocol approved by the Animal Research Committee of this institution.

Protein assay

Protein concentrations were determined by means of the Bradford method using protein assay dye solution (Bio-Rad).

GST activity assay

GST activity was assayed in the presence of 1 mM glutathione, 1 mM CDNB, and 100 mM potassium phosphate (pH 6.5) at 37 °C by continuously monitoring the increase in absorbance at 340 nm. The molar absorption coefficient of glutathione conjugated CDNB was 9,600. One unit is defined for the amount of enzyme required to catalyze the conjugation of 1 μmol of CDNB/min.

Production in Escherichia coli and purification of recombinant GST

A plasmid carrying the GST gene from *S. japonicum* (pGEX-4T-1, Amersham Bioscience) was used for the transformation of *E. coli* DH5α. The gene has a *tac* promoter inducible by IPTG. After the induction of GST by IPTG, the cells were collected by centrifugation and suspended in 10 ml of 150 mM NaCl, 1 mM EDTA, and 50 mM Tris–HCl, pH 8.0. After sonication three times for 10 s each on ice, the homogenate was centrifuged at 15,000 rpm for 30 min. The soluble fraction was collected and applied to a glutathione–Sepharose 4B column equilibrated with 140 mM NaCl and 40 mM phosphate buffer, pH 7.3, followed by washing with the same buffer. Bound proteins were eluted from the column by 10 mM GSH in 50 mM Tris–HCl, pH 8.0, and dialyzed in 40 mM NaCl and 40 mM phosphate buffer, pH 7.3, overnight at 4 °C to remove GSH.

Biotinylation of GST

Since a significant fraction of the GST activity is abolished during the biotinylation reaction, to protect the glutathione binding site of GST, biotin labeling was performed using GST bound to the glutathione–Sepharose 4B resin. GST was mixed with 1 ml of glutathione–Sepharose 4B and incubated for 30 min at room temperature. The GST-bound resin was collected by centrifugation and labeled with biotin according to manufacturer's instruction. The reaction was terminated by adding 0.1 ml of 1 M Tris–HCl, pH 8.0. After placing the mixture on the column, it was washed with 30 ml buffer and eluted with 10 mM GSH in 50 mM Tris–HCl, and dialyzed at 4 °C overnight.

Glutathionylation of bovine serum albumin and ovalbumin

Since bovine serum albumin (BSA) has a limited number of sulfhydryl group that can be S-glutathionylated, the disulfide bonds were reduced in the first step. BSA, dissolved in PBS, was denatured by treatment with 0.1% SDS and reduced with 5 mM dithiothreitol (DTT) for 5 min in boiling water. DTT and excess SDS were removed by a PD-10 desalting column. Either GSH or GSSG was added to 1 mM to the reduced BSA or ovalbumin (OVA). To affect oxidation, 2.5 mM diamide or 100 mM hydrogen peroxide was added followed by incubation for 15 min at 37 °C. Excess glutathione and hydrogen peroxide were removed by passing the solution through the PD-10 column again. OVA was also reduced and S-glutathionylated with 25 mM GSH and 200 mM hydrogen peroxide in the same manner as was used for BSA.

Cell culture

HeLa cells were maintained in Dulbecco's modified minimum essential medium (DMEM; Sigma) containing 100 U/ml penicillin and 100 μg/ml streptomycin supplemented with 10% fetal bovine serum (FBS; Invitrogen). Cells were grown at 37 °C in a humidified atmosphere with 5% CO_2.

Preparation and S-glutathionylation of cellular proteins

After washing twice with PBS, the cells were scraped, collected by centrifugation, and disrupted by sonication in PBS. After centrifugation at 15,000 rpm for 20 min in a microcentrifuge, the soluble fraction was collected and stored at −20 °C until use. S-Glutathionylation was performed by incubation with agents at 37 °C under indicated conditions.

SDS–PAGE and blotting to nitrocellulose membranes

Protein samples (20 μg/lane) were subjected to 10% SDS–PAGE under non-reducing conditions. The separated proteins were then either stained with Coomassie brilliant blue G-250 or transferred to a Hybond nitrocellulose membrane (Amersham–Pharmacia) under semi-dry conditions using a transfer-blot SD semi-dry transfer cell (Bio-Rad).

Detection of S-glutathionylated proteins by biotin–GST on blotted membrane

The membranes were blocked by incubation with 5% BSA in PBS for 2 h at room temperature and further incubated with 30 μg/ml biotin–GST overnight. After washing with PBS containing 0.1% Tween 20 for 10 min by changing buffer three times, they were reacted with HRP-conjugated streptavidin (1:1000 dilution) for 1 h at room temperature. Peroxidase activity was detected after treatment with 2 mM hydrogen peroxide and 0.6 mg/ml 4-chloro-1-naphthol in PBS.

Histochemical detection of glutathionylated proteins in rat tissues

Tissues, obtained from rats killed under anesthesia with diethyl ether, were immediately fixed in Bouin solution for histochemical study. After embedding in paraffin, 4 μm sections were prepared and mounted on silan-coated glass plates. After deparaffinization and rehydration, the tissue sections were subjected to autoclaving for 10 min to increase reactivity to GST and then treated with 1% porcine serum for 10 min to block nonspecific binding. They were incubated with biotin–GST (30 μg/ml) at room temperature for 2 h, washed, and then reacted with HRP-conjugated streptavidin (1:1000 dilution; Santa Cruz) for 1 h. After a final rinse, labeling was examined using 3,3′-diaminobenzidine (Envision kit HRP(DAB), Dako, Japan) as the chromogen, which was placed on the tissues for a few minutes. To examine the specificity of the positive staining, sections were incubated without biotin–GST or reacted with biotin–GST in the presence of S-glutathionylated OVA and then proceeded to the following reaction. Photographs were taken with a digital camera under a light microscope (Olympus BX50, Tokyo, Japan).

Preparation of mouse tissue samples

Three pairs of hetero SOD1-knockout mice, established by Matzuk et al. [27], were purchased through the Jackson Laboratories (Bar Harbor, ME) and bred in our institute. Fresh tissues were dissected from mice under anesthesia with diethyl ether and immediately frozen in liquid nitrogen. They were powdered in a mortar under liquid nitrogen. After homogenization in PBS and centrifugation at 15,000 rpm for 20 min, soluble fractions were used in the detection of S-glutathionylated proteins.

Results

Detection of S-glutathionylated BSA by biotin–GST

Glutathione *S*-transferase (GST) from *S. japonicum* binds glutathione with high affinity and is often used to detect GST-fusion proteins expressed as recombinant proteins in cells. Another merit to use GST from *S. japonicum* is the availability of specific antibody against it. The antibody is specific to *S. japonicum* GST, although GST is present ubiquitously in living organisms. We established a simple method to detect glutathionylated proteins by employing binding ability of GST to the glutathione moiety of the S-glutathionylated proteins. Labeling of GST with biotin made it possible to detect bound GST using HRP-conjugated streptavidin.

We first examined whether or not S-glutathionylation could be detected by biotin-labeled GST using S-glutathionylated BSA in vitro (Fig. 1). BSA was first reduced with DTT, incubated with GSH, GSSG, or GSNO with or without oxidation by diamide. The BSA on each lane showed a slightly different mobility on gels (Fig. 1B). This can be attributed to a conformation that is unique to each redox state of BSA since, when it is separated on a reducing gel, no such shift was detected (data not shown). This GST-overlay method detected the BSA that had been reacted with GSH, with or without oxidation by diamide, or GSNO (Fig. 1A). Diamide alone showed no band on the blot. The presence of GSSG increased the positive band only slightly.

Detection of S-glutathionylated proteins in cellular extract by GST

We then applied the method to the detection of S-glutathionylation in proteins extracted from HeLa cells. A soluble extract was prepared from HeLa cells and subjected to the biotin–GST-overlay method (Fig. 2). Numerous proteins were found to be S-glutathionylated,

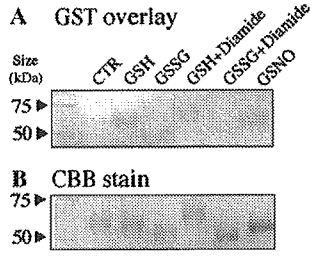

Fig. 1. Detection of the glutathionylation in BSA by biotin–GST overlay followed by treatment with HRP-streptavidin. BSA was reduced and immediately incubated with the agents indicated. After SDS–PAGE, the proteins were either blotted onto a nitrocellulose membrane (A) or stained with Coomassie brilliant blue G-250 (B). The blot was overlaid with biotin–GST and incubated overnight, followed by the reaction with HRP-streptavidin and visualization of the bands. The details of experiments are described under Materials and methods. Typical data from several experiments are shown.

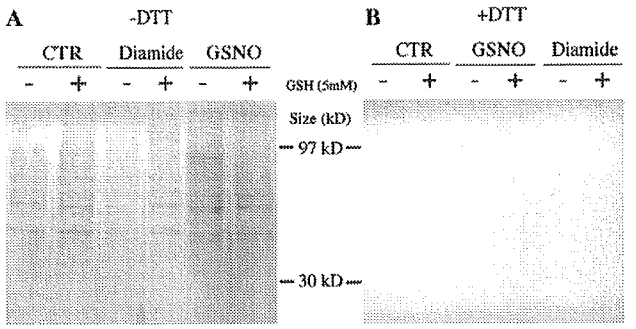

Fig. 2. Detection of S-glutathionylated proteins on blots by the biotin–GST-overlay method. Soluble protein extracts were prepared from HeLa cells and were incubated under the indicated conditions for 1 h at 37 °C. Proteins (20 μg) were separated on 10% SDS–PAGE, and were blotted onto nitrocellulose membranes. (A) The membranes were subjected to the biotin–GST-overlay method. (B) To evaluate the specificity of the method, the blot membrane was incubated with 10 mM DTT for 1 h at 37 °C and then subjected to the biotin–GST-overlay method. Typical data from several experiments are shown.

even in untreated cells (Fig. 2A). The resulting bands were elevated by treatment of the cell extracts with either GSNO or GSH plus diamide, as found in the BSA. GSNO alone enhanced the S-glutathionylation reaction that was decreased by the presence of GSH. Diamide enhanced the reaction only when GSH was present. This is consistent with previous reports in which ^{35}S was employed to detect S-glutathionylated proteins [20]. Diamide-induced oxidation in the presence of GSH showed different profiles for S-glutathionylation from the other treatments, especially in the high molecular weight range. This could be caused by the harsh oxidative potential of diamide. The specificity of the method to S-glutathionylated proteins was assessed using membranes that had been pretreated with 250 mM of 2-mercaptoethanol (data not shown) or 10 mM DTT for 1 h at 37 °C (Fig. 2B). These treatments reduced the disulfide bonds and released the bound GSH. No band was observed after the reduction, and this loss of staining confirms the specificity of this method for detecting S-glutathionylated proteins. We also attempted to use an anti-GST antibody to detect GST bound to S-glutathionylated proteins. Although similar sized bands were detected, several bands remained on the reduced blot with DTT (data not shown). This would be due to non-specific binding of the antibody. Hence, we chose the biotin–GST to detect S-glutathionylation in subsequent studies.

Characterization of GSNO-dependent S-glutathionylation

Since GSNO is a well-known mediator of the S-glutathionylation reaction [6], we further characterized GSNO-dependent S-glutathionylation using the GST-overlay method. When cellular proteins were incubated in the presence of various concentrations of GSNO, the

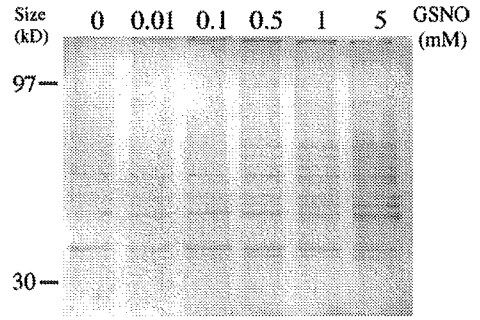

Fig. 3. Dose effects of GSNO-dependent S-glutathionylation. Soluble protein extracts were first incubated with various concentrations of GSNO for 1 h at 37 °C, and then subjected to detection of S-glutathionylation by the biotin–GST-overlay method. Typical data from several experiments are shown.

extent of S-glutathionylation of proteins correlated with GSNO concentration (Fig. 3). Although the intensity of each band increased, the positions of the signals were not altered. Thus, GSNO enhanced only the S-glutathionylation reaction of susceptible proteins.

Effects of several agents on S-glutathionylation in cells

We then examined effects of agents that either affect the intracellular redox state or become sources of ROS/RNOS on the levels of S-glutathionylated proteins in HeLa cells (Fig. 4). The concentrations used are ones commonly used in this kind of experiments. After incubating the cells with these agents for an appropriate period, soluble proteins were prepared and subjected to the GST-overlay method to detect S-glutathionylated proteins. All of these agents stimulated S-glutathionylation under these conditions. Although oxidation by diamide resulted in a unique profile of S-glutathionylation in cell-free samples, as shown in Fig. 2, a similar profile of S-glutathionylated proteins to other stimuli was observed in the cells. It is noteworthy that NAC, a reducing agent, and BSO, a glutathione-depleting agent, also enhanced the S-glutathionylation of cellular proteins.

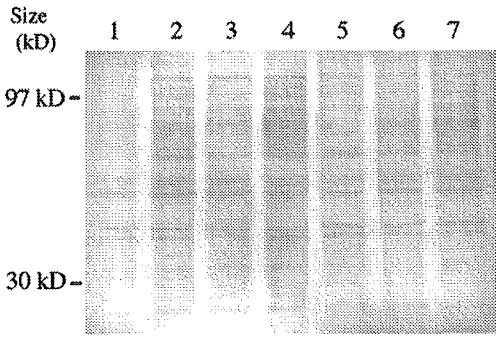

Fig. 4. Comparison of the effects of several agents on the formation of S-glutathionylated proteins in cells. HeLa cells were incubated under control conditions (lane 1) or with 1 mM diamide (30 min, lane 2), 1 mM hydrogen peroxide (30 min, lane 3), 5 mM GSNO (30 min, lane 4), 1 mM BCNU (24 h, lane 5), 5 mM BSO (24 h, lane 6), or 20 mM NAC (24 h, lane 7) at 37 °C. Soluble proteins were prepared and subjected to the GST-overlay method. Typical data from several experiments are shown.

Histochemical detection of S-glutathionylated proteins in tissues

We then attempted to detect glutathionylated proteins in tissue sections from several rat organs. The application of biotin–GST to tissue sections clearly permitted positive staining to be detected (Fig. 5). Although some proteins endogenously contain biotin, staining found without biotin–GST was very weak, compared with positive signals, and can be considered negligible (data not shown). When S-glutathionylated OVA was present during an incubation with biotin–GST, the signal became very faint. This suggests that most signals were derived from biotin–GST bound specifically to S-glutathionylated proteins. Thus, the GST-overlay method is also applicable to in situ detection of S-glutathionylation. In the preliminary study, epithelia of uterus, oviduct, and granulose cells among rat female reproductive tissues were strongly stained by this method. Epithelial cells of some other tissues, such as the epididymis and renal tubules in the kidney, also showed strong staining (data not shown).

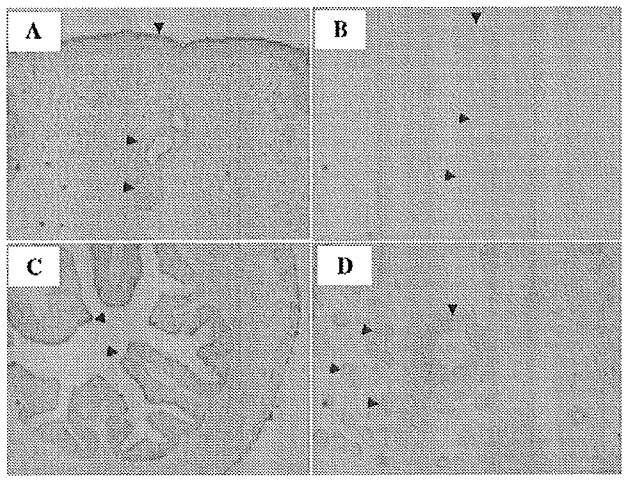

Fig. 5. Histochemical detection of S-glutathionylated proteins by biotin–GST in rat female reproductive tissues. GST overlay was applied to the in situ detection of S-glutathionylated proteins on sections from rat female reproductive tissues. After reaction with biotin–GST 2 h at room temperature and washing with PBS, tissue sections were treated with HRP-conjugated streptavidin for 1 h and washed. An Envision kit HRP(DAB) was used to visualize the reactive materials. Typical data from several experiments were shown. Magnification, 260×. (A, B) Uterus. Black arrowhead, surface epithelia; blue arrowhead, endometrial gland. For evaluating specificity of the reaction, S-glutathionylated OVA was included during incubation with biotin–GST (B). (C) Oviduct. Black arrowhead, epithelial cells. (D) Ovary. Black arrowhead, granulosa cells; blue arrowhead, primordial follicle.

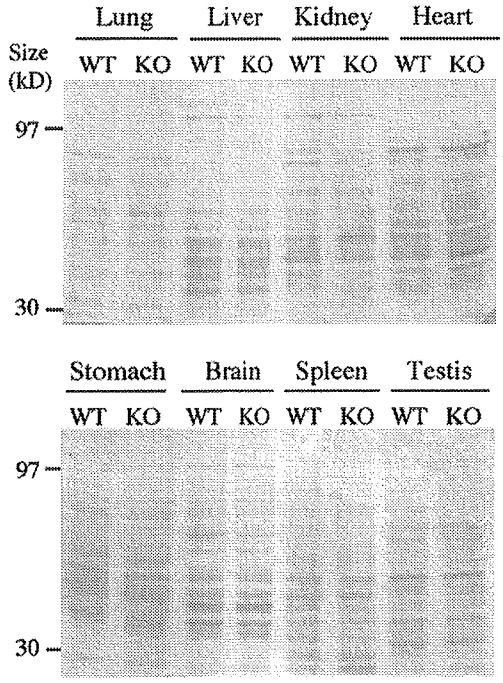

Fig. 6. Levels of S-glutathionylated proteins in SOD1-knockout and wild-type mouse tissues. Tissue homogenates were prepared from SOD1-knockout (KO) and wild-type (WT) mouse organs, separated by SDS–PAGE, and blotted onto nitrocellulose membranes. The biotin–GST overlay was performed to detect glutathionylated proteins on the membranes.

Tissue levels of S-glutathionylated proteins in mice

To determine the tissue distribution of S-glutathionylation, we prepared proteins from eight tissues from wild-type mice. Since oxidative stress and, hence, protein S-glutathionylation may be increased in SOD1-knockout mouse, proteins were also prepared from SOD1-knockout mouse. They were subjected to the GST-overlay method (Fig. 6). Numerous protein bands were detected in all tissues examined. S-Glutathionylation occurred in manners specific to each tissue, implying that proteins that are susceptible to S-glutathionylation are unique to individual tissues. Unexpectedly, no significant difference was observed between the SOD1-knockout and wild-type mice. This is, however, consistent with healthily growing knockout mice under clean, specific pathogen free (SPF) breeding conditions.

Discussion

Oxidative and nitrosative stress cause the modification of proteins and impair their biological function. Among the amino acids found in proteins, cysteine is the most susceptible to modification by ROS and RNOS. Glutathione is present in the millimolar range in cells and prevents reactive sulfhydryls from oxidative modification. The resulting GSSG is recycled by glutathione reductase that is present ubiquitously and especially abundant in the epithelia of ductal tissues [28–30]. It has been known for more than 50 years that glutathione also reacts with other thiol compounds, including proteins, and forms mixed disulfides. The physiological significance of this reaction has, however, been recognized only recently [6]. This occurs coincidentally with an increase in studies of the consequences of ROS and RNOS. It is now generally accepted that a significant aspect of sulfhydryl modification is related to S-glutathionylation [2]. Since studies of the physiological function of S-glutathionylation have just begun, many issues remain to be answered [6]. A novel function of S-glutathionylation is the requirement for the activation of the antioxidative enzyme 1-Cys peroxiredoxin [14]. Numerous proteins were found to be S-glutathionylated in vivo in a tissue-specific manner, but the physiological meaning of the modification has awaited clarification.

The mechanism by which S-glutathionylation occurs in cells is largely unknown. To elucidate the mechanism and physiological roles of the S-glutathionylation reaction, a convenient assay method that reflects the modification is needed. Several methods have been developed and applied to the detection of sulfhydryl modification. The metabolic labeling of glutathione with a radioisotope, ^{35}S, is the most common method, but sometimes problems are encountered [20]. Other methods also have drawbacks associated with difficulty in handling and from the quantitative point of view. In addition, an evaluation of S-glutathionylated proteins in vivo is impossible by such methods. The identification of S-glutathionylated proteins by anti-GSH antibody has recently been reported [31]. However, the antibody also reacted with reduced proteins, suggesting that the specificity was not very high. The utilization of antibodies with an ambiguous specificity may cause false positive bands, leading to erroneous results. A simple and quantitative method, that is capable of detecting S-glutathionylated proteins in situ and which can be performed in any laboratory is still awaited. We describe here the establishment of a rather simple method using GST originated from *S. japonicum*. Although the binding ability of GST to S-thiolated glutathione is lower than to free GSH, it was able to detect the glutathione moiety in proteins sufficiently.

We first tested this method in a simple system using BSA incubated with GSH, GSSG, or GSNO in the absence or presence of diamide. While GSH alone stimulated the S-glutathionylation of BSA, GSSG did not (Fig. 1). Although a thiol–disulfide exchange is one of the postulated mechanisms for the S-glutathionylation of proteins, it appears that it was not efficient under these experimental conditions. A similar conclusion was obtained when human neutrophil proteins [32] and actin [26] were used as target proteins for S-glutathionylation. The thiol–disulfide exchange reaction is accelerated in the

presence of high concentrations of GSSG and at alkaline pH, but the S-glutathionylation by GSSG may not be the major contributor under physiological conditions with very low concentrations of GSSG and at a neutral pH.

The application of this method to proteins isolated from cultured cells exhibited numerous bands on the blot membrane that were totally abolished by treatment with DTT (Fig. 2). This indicates that the reduction of disulfide bonds released glutathione. Thus, bands detected by this method were mainly derived from S-glutathionylated proteins. These data indicate that a significant fraction of the proteins were S-glutathionylated in the cells under conventional culture conditions. Since oxygen concentrations in a CO_2 incubator are higher than most normal tissues in vivo, cells are constitutively exposed to hyperoxic conditions when in such a culture. This would enhance the S-glutathionylation of cellular proteins. Even though, S-glutathionylation in cultured cells would still reflect, at least in part, the in vivo state because many proteins were found to be S-glutathionylated in extracts from tissues of mice (Fig. 6).

In situ detection of S-glutathionylation would be a powerful tool, in terms of understanding the physiological role of the reaction. The method established here is simple and quite similar to the immunological method and, hence, is applicable for use with tissue sections as well as protein-blotted membranes. In the preliminary histochemical study (Fig. 5), we found that S-glutathionylation preferentially occurred in tissues that express high levels of glutathione reductase [29,30], except for some cells such as granulosa cells. A high recycling activity of GSSG is required for tissues that are under constitutive oxidative stress and many epithelial tissues would fit this criterion.

Treatment of cellular extracts with GSNO led to an increase in intensity of bands in a dose-dependent manner, but excess GSH suppressed the reaction (Figs. 2 and 3). It is likely that this is due to a shift in the reaction to form GSSG, as the result of the presence of GSH. GSNO is a well-known S-glutathionylating agent [2]. The actual active species is not GSNO, but its decomposition product, glutathione disulfide S-oxide [33–35]. Formation of glutathione disulfide S-oxide is believed to involve the sulfenic acid and thiosulfinamide that are generated by reaction of GSH with ROS and RNOS in cells [34]. On the other hand, it has been proposed that sulfenic acid is an intermediate in the formation of disulfides in BSA that had been treated with either hydrogen peroxide or peroxynitrite [36]. However, the mechanism of S-glutathionylation by other stimuli is not clear as of this writing.

While diamide alone had either no effect or slightly decreased staining of band, the presence of GSH increased the levels of S-glutathionylated proteins. This would be due to the fact that a fairly large amount of glutathione is required for the S-glutathionylation of proteins. The profile for the positive bands that appeared in the presence of GSH and diamide was quite different from either the original bands or a GSNO-treated sample. Since diamide is a strong oxidant, excess disulfide bonds would be formed by the harsh oxidation of proteins. The treatment of cultured cells with diamide, however, showed profile that was similar to the other stimuli (Fig. 4). Although diamide is frequently used as an oxidant in studies of S-glutathionylation, this suggests that special care will be needed for studies in which isolated proteins are used.

Unexpectedly, treatment of cells with BSO, BCNU, or NAC also stimulated the S-glutathionylation reaction. Both BSO and BCNU are commonly used to reduce intracellular free glutathione. These data, however, indicate that a significant portion of the glutathione forms a mixed disulfide with proteins in cells. Both the inhibition of glutathione biosynthesis and recycling would cause oxidative stress and elevate glutathionylation. The enhanced S-glutathionylation by NAC may be explained by the elevation in glutathione levels by augmented glutathione biosynthesis. NAC is generally used to increase intracellular glutathione. However, elevation in the level of glutathione may increase population that binds proteins. Although NAC is a well-known antioxidant, based on in vitro experiments, prooxidant capability of NAC and GSH has been reported [37]. BSO inhibits glutathione synthesis by inhibiting γ-glutamylcysteine synthetase, a rate-determining enzyme of glutathione synthesis. BCNU, on the other hand, inhibits glutathione reductase, resulting in inhibition of recycling of oxidized glutathione (GSSG). Thus, both BSO and BCNU decrease levels of intracellular glutathione. Since GSH plays a major role in maintaining intracellular redox state, lowering GSH levels causes oxidative stress. Thus, the enhanced glutathionylation might occur during the process of GSH depletion. Further examination would be required to clarify this.

Conclusions

The use of GST as a probe for detecting S-glutathionylated proteins was found to be a simple and sensitive method. This method is applicable to proteins on blots as well as tissues sections. The identification of individual proteins in each tissue is required if the functional consequence of S-glutathionylation is an issue. Owing to its simplicity and sensitivity, the GST-overlay method represents a potentially powerful tool in proteomics for investigating S-glutathionylated proteins in vivo.

Acknowledgments

This work was supported, in part, by Grant-in-Aid for Scientific Research (C) (No. 16590238) and 21st Century COE Program from Japan Society for the

Promotion of Science (JSPS) and by the Cosmetology Research Foundation.

References

[1] B. Halliwell, J.M.C. Gutteridge, Free Radical Biology and Medicine, third ed., Clarendon Press, Oxford, 1999.
[2] C.M. Padgett, A.R. Whorton, Arch. Biochem. Biophys. 358 (1998) 232–242.
[3] P. Klatt, E.P. Molina, S. Lamas, J. Biol. Chem. 274 (1999) 15857–15864.
[4] K. Itoh, K.I. Tong, M. Yamamoto, Free Radic. Biol. Med. 36 (2004) 1208–1213.
[5] J.A. Thomas, B. Poland, R. Honzatko, Arch. Biochem. Biophys. 319 (1995) 1–9.
[6] P. Klatt, S. Lamas, Eur. J. Biochem. 267 (2000) 4928–4944.
[7] K.P. Huang, F.L. Huang, Biochem. Pharmacol. 64 (2002) 1049–1056.
[8] S. Mohr, H. Hallak, A. de Boitte, E.G. Lapetina, B. Brune, J. Biol. Chem. 274 (1999) 9427–9430.
[9] A. Chandra, S. Srivastava, J.M. Petrash, A. Bhatnagar, S.K. Srivastava, Biochemistry 36 (1997) 15801–15809.
[10] J.F. Caplan, N.R. Filipenko, S.L. Fitzpatrick, D.M. Waisman, J. Biol. Chem. 279 (2004) 7740–7750.
[11] N.E. Ward, D.S. Pierce, S.E. Chung, K.R. Gravitt, C.A. O'Brian, J. Biol. Chem. 273 (1998) 12558–12566.
[12] E. Cabiscol, R.L. Levine, Proc. Natl. Acad. Sci. USA 93 (1996) 4170–4174.
[13] L.M. Landino, K.L. Moynihan, J.V. Todd, K.L. Kennett, Biochem. Biophys. Res. Commun. 314 (2004) 555–560.
[14] Y. Manevich, S.I. Feinstein, A.B. Fisher, Proc. Natl. Acad. Sci. USA. 101 (2004) 3780–3785.
[15] Y.C. Chai, C.H. Jung, C.K. Lii, S.S. Ashraf, S. Hendrich, B. Wolf, H. Sies, J.A. Thomas, Arch. Biochem. Biophys. 284 (1991) 270–278.
[16] S.A. Gravina, J.J. Mieyal, Biochemistry 32 (1993) 3368–3376.
[17] S. Yoshitake, H. Nanri, M.R. Fernando, S. Minakami, J. Biochem. 116 (1994) 42–46.
[18] C.H. Jung, J.A. Thomas, Arch. Biochem. Biophys. 335 (1996) 61–72.
[19] M. Fratelli, H. Demol, M. Puype, S. Casagrande, I. Eberini, M. Salmona, V. Bonetto, M. Mengozzi, F. Duffieux, E. Miclet, A. Bachi, J. Vandekerckhove, E. Gianazza, P. Ghezzi, Proc. Natl. Acad. Sci. USA 99 (2002) 3505–3510.
[20] I.A. Cotgreave, R.G. Gerdes, Biochem. Biophys. Res. Commun. 242 (1998) 1–9.
[21] D.M. Sullivan, N.B. Wehr, M.M. Fergusson, R.L. Levine, T. Finkel, Biochemistry 39 (2000) 11121–11128.
[22] C. Lind, R. Gerdes, Y. Hamnell, I. Schuppe-Koistinen, H.B. von Lowenhielm, A. Holmgren, I.A. Cotgreave, Arch. Biochem. Biophys. 406 (2002) 229–240.
[23] M. Hirose, T. Hayano, H. Shirai, H. Nakamura, M. Kikuchi, Protein Eng. 11 (1998) 243–248.
[24] O.P. Hjelle, F.A. Chaudhry, O.P. Ottersen, Eur. J. Neurosci. 6 (1994) 793–804.
[25] T. Soderdahl, M. Enoksson, M. Lundberg, A. Holmgren, O.P. Ottersen, S. Orrenius, G. Bolcsfoldi, I.A. Cotgreave, FASEB J. 17 (2003) 124–126.
[26] I. Dalle-Donne, R. Rossi, D. Giustarini, R. Colombo, A. Milzani, Free Radic. Biol. Med. 35 (2003) 1185–1193.
[27] M.M. Matzuk, L. Dionne, Q. Guo, T.R. Kumar, R.M. Lebovitz, Endocrinology 139 (1998) 4008–4011.
[28] T. Fujii, R. Hamaoka, J. Fujii, N. Taniguchi, Arch. Biochem. Biophys. 378 (2000) 123–130.
[29] T. Kaneko, Y. Iuchi, S. Kawachiya, T. Fujii, H. Saito, H. Kurachi, J. Fujii, Biol. Reprod. 65 (2001) 1410–1416.
[30] T. Kaneko, Y. Iuchi, T. Kobayashi, T. Fujii, H. Saito, H. Kurachi, J. Fujii, Eur. J. Biochem. 269 (2002) 1570–1578.
[31] J. Craghill, A.D. Cronshaw, J.J. Harding, Biochem. J. 379 (2004) 595–600.
[32] Y.C. Chai, S.S. Ashraf, K. Rokutan, R.B. Johnston Jr., J.A. Thomas, Arch. Biochem. Biophys. 310 (1994) 273–281.
[33] Y. Ji, T.P. Akerboom, H. Sies, J.A. Thomas, Arch. Biochem. Biophys. 362 (1999) 67–78.
[34] J. Li, F.L. Huang, K.P. Huang, J. Biol. Chem. 276 (2001) 3098–3105.
[35] L. Tao, A.M. English, Biochemistry 43 (2004) 4028–4038.
[36] S. Carballal, R. Radi, M.C. Kirk, S. Barnes, B.A. Freeman, B. Alvarez, Biochemistry 42 (2003) 9906–9914.
[37] M.L. Sagrista, A.E. Garcia, M. Africa De Madariaga, M. Mora, Free Radic. Res. 36 (2002) 329–340.

An abortive apoptotic pathway induced by singlet oxygen is due to the suppression of caspase activation

Kaoru OTSU*, Kazuaki SATO†, Yoshitaka IKEDA‡, Hirotaka IMAI§, Yasuhito NAKAGAWA§, Yoshihiro OHBA† and Junichi FUJII*[1]

*Department of Biomolecular Function, Graduate School of Medical Science, Yamagata University, 2-2-2 Iidanishi, Yamagata 990-9585, Japan, †Department of Chemical Engineering, Faculty of Engineering, Yamagata University, 4-3-16 Jonan, Yonezawa 992-8510, Japan, ‡Division of Molecular Cell Biology, Department of Biomolecular Sciences, Saga University Faculty of Medicine, 5-1-1 Nabeshima, Saga 849-8501, Japan, and §School of Pharmaceutical Sciences, Kitasato University, 5-9-1 Shirokane, Minato-ku, Tokyo 108-8641, Japan

Singlet oxygen causes the cytotoxic process of tumour cells in photodynamic therapy. The mechanism by which singlet oxygen damages cells is, however, not fully understood. To address this issue, we synthesized and used two types of endoperoxides, MNPE (1-methylnaphthalene-4-propionate endoperoxide) and NDPE (naphthalene-1,4-dipropionate endoperoxide), that generate defined amounts of singlet oxygen at 37 °C with similar half lives. MNPE, which is more hydrophobic than NDPE, induced the release of cytochrome *c* from mitochondria into the cytosol and exhibited cytotoxicity, but NDPE did not. RBL cells, a rat basophil leukaemia-derived line, that overexpress phospholipid hydroperoxide glutathione peroxidase in mitochondria were found to be highly resistant to the cytotoxic effect of MNPE. MNPE treatment induced much less DNA ladder formation and nuclear fragmentation in cells than etoposide treatment, even though these treatments induced a similar extent of cellular damage. Singlet oxygen inhibited caspase 9 and 3 activities directly and also suppressed the activation of the caspase cascade. Collectively, these data suggest that singlet oxygen triggers an apoptotic pathway by releasing cytochrome *c* from mitochondria via the peroxidation of mitochondrial components and results in cell death that is different from typical apoptosis, because of the abortive apoptotic pathway caused by impaired caspase activation.

Key words: apoptosis, caspase, cytochrome *c*, endoperoxide, singlet oxygen.

INTRODUCTION

ROS (reactive oxygen species) are produced during various biological process, such as inflammation and aging, and result in the dysfunction of susceptible cells [1]. Considerable efforts have been made to comprehend the mechanism of damage, including apoptosis, by ROS. In the intrinsic apoptotic pathway, ROS commonly triggers the release of cytochrome *c* from mitochondria into the cytosol [2,3]. The released cytochrome *c*, together with dATP and magnesium ions, stimulates protein factors, including Apaf-1 and procaspase 9, to form an apoptosome, resulting in proteolytic activation of the caspase cascade [4]. At a later stage, procaspase 3 is converted into the active form by the activated caspase 9, cleaves protein components, such as ICAD [inhibitor of caspase-dependent proteinase CAD (caspase-activated DNase)] and PARP [poly(ADP-ribose) polymerase], and leads to DNA fragmentation. From morphological points of view, chromatin condensation and nuclear fragmentation occur during apoptosis.

The hydroxyl radical, which is produced from H_2O_2 via a one-electron reduction, is regarded as the most reactive and, hence, is an extremely detrimental ROS. Singlet oxygen is produced during photochemical reactions in the presence of a photosensitizer. Superoxide-mediated radical reactions [5] and the decomposition of peroxynitrite [6] may also be sources of singlet oxygen.

Singlet oxygen is assumed to cause skin photoaging [7] and the cytotoxic process for tumour cells during photodynamic therapy [8]. Singlet oxygen kills bacteria [9–11] and is utilized to exterminate viruses without adverse effects [12]. When viruses are exposed to singlet oxygen, infection is prohibited without causing viral DNA damage. NAD(P)H appears to be one of primary targets of singlet oxygen in mitochondria [13]. Since proteins are present at high concentrations in the body and contain reactive residues, such as tryptophan, tyrosine, histidine and cysteine, approx. 68 % of singlet oxygen is consumed by proteins [14].

Singlet oxygen produced by UVA irradiation is known to induce apoptosis in T-cells [15,16] and HL-60 cells [17]. Singlet oxygen and UV activate mitogen-activated protein kinases, p38, JNK (c-Jun N-terminal kinase) and ERK (extracellular-signal-regulated kinase) [18–20]. Singlet oxygen, as well as H_2O_2, result in the cleavage of Bid, which causes the release of cytochrome *c* from mitochondria. Zhuang et al. [21] compared the effects of singlet oxygen and H_2O_2, and concluded that singlet oxygen activates both the p38- and caspase-8-mediated pathways, but H_2O_2 activates only the caspase-8-mediated pathway. Despite its significant role in photoaging and for therapeutic purposes, the biological effects of singlet oxygen, especially on proteins, are poorly characterized. One of reasons is that an adequate system for producing pure singlet oxygen quantitatively is barely available.

We synthesized water-soluble endoperoxides that enabled us to investigate the function of singlet oxygen in biological systems. In the present paper, we report that singlet oxygen produced within cells is highly toxic and causes cell death. Although the release of cytochrome *c* from mitochondria was observed, cell death did not show the typical profile of apoptosis mainly due to the suppression of caspases by singlet oxygen.

Abbreviations used: BHT, butylated hydroxytoluene; BSO, L-buthionine sulphoximine; DABCO, 1,4-diazadicyclo[2.2.2]octane; DAPI, 4,6-diamidino-2-phenylindole; DMEM, Dulbecco's modified minimum essential medium; DTT, dithiothreitol; ERK, extracellular-signal-regulated kinase; FBS, foetal bovine serum; GPx, glutathione peroxidase; JNK, c-Jun N-terminal kinase; LDH, lactate dehydrogenase; MCA, methyl-coumaryl-7-amide; MNP, 1-methylnaphthalene-4-propionate; MNPE, 1-methylnaphthalene-4-propionate endoperoxide; NDP, naphthalene-1,4-dipropionate; NDPE, naphthalene-1,4-dipropionate endoperoxide; PARP, poly(ADP-ribose) polymerase; PHGPx, phospholipid hydroperoxide GPx; ROS, reactive oxygen species; SNAP, *S*-nitroso-*N*-acetyl-D,L-penicillamine; SOD, superoxide dismutase; TBS, Tris-buffered saline; THF, tetrahydrofuran; WST-1, 2-(4-iodophenyl)-3-(4-nitrophenyl)-5-(2,4-disulphophenyl)-2*H*-tetrazolium.

[1] To whom correspondence should be addressed (email jfujii@med.id.yamagata-u.ac.jp).

EXPERIMENTAL

Materials

MNPE (1-methylnaphthalene-4-propionate endoperoxide) and NDPE (naphthalene-1,4-dipropionate endoperoxide) were synthesized as described previously [22]. The structure and purity of the endoperoxides were determined by NMR. The half-lives of MNPE and NDPE were approx. 25 min and 27 min at 37 °C respectively. The generation of singlet oxygen from endoperoxides was detected by ESR using DRD156 [4,4′-bis(1-*p*-carboxyphenyl-3-methyl-5-hydroxyl)pyrazole] as a sensitive singlet-oxygen-detecting probe, which specifically reacts with singlet oxygen among the ROS [23]. The efficiency of singlet oxygen formation was similar between MNPE and NDPE, although reported yield varies from 45 to 98 %, depending on the assay methods used [24,25]. Vitamin E, vitamin E succinate, DABCO (1,4-diazadicyclo[2.2.2]octane) and β-carotene were purchased from Sigma.

Cell culture

HepG2 cells were maintained in DMEM (Dulbecco's modified minimal essential medium) (Sigma) containing 100 units/ml penicillin and 100 μg/ml streptomycin supplemented with 10 % FBS (foetal bovine serum) (Invitrogen). RBL cells, a rat basophil leukaemia-derived line, and their transfectants were maintained in DMEM containing the above antibiotics supplemented with 5 % FBS and 0.5 mg/ml geneticin (Gibco BRL). Cells were grown at 37 °C in a humidified atmosphere containing 5 % CO_2.

HPLC analysis of MNP (1-methylnaphthalene-4-propionate) and NDP (naphthalene-1,4-dipropionate) in cells

The delivery of endoperoxides to cells was assessed by measuring decomposition products, MNP and NDP, as described by Klotz et al. [19]. After incubation with 2 mM MNPE or NDPE for 2 h, HepG2 cells (1×10^7) were washed with PBS and scraped. Cells were disrupted for 1 min by a Bioruptor (Cosmo Bio, Tokyo, Japan) at 200 W with cooling in ice-cold water. The sample was centrifuged at 15000 *g* for 10 min followed by centrifugation at 100000 *g* for 60 min. The supernatant was partially deproteinized by Microcon (cut-off molecular mass 30 kDa) (Millipore) and subjected to HPLC (LC-2000; Jasco) on a reversed-phase C_{18} column (Toso, Tokyo, Japan). The decomposition product, MNP or NDP, was eluted at 25 °C at a flow rate of 1 ml/min. The mobile phase was methanol/50 mM ammonium acetate, pH 7.0, with 20 % methanol for 1 min, increased to 100 % methanol in 9 min, and was kept at 100 % methanol for 5 min. Absorbance of the eluent was monitored at 290 nm. Amounts of the decomposed compounds that had been incorporated into cells were standardized based on the recovery of a known amount of MNP or NDP added to the supernatant prepared from untreated control cells.

HPLC analysis of vitamin E in cells

The delivery of vitamin E or vitamin E succinate into cells was determined according to the method described in [26]. After incubation with 10 μM vitamin E or vitamin E succinate for 16 h, the cells (1×10^7) were washed with PBS, scraped and suspended into 100 μl of PBS containing 0.01 % BHT (butylated hydroxytoluene). The cell suspension was mixed with 500 μl of n-hexane. After 2 min, this mixture was deproteinized with cool ethanol, denatured with 5 % methanol, and vortex-mixed for 5 min. The upper phase was separated after centrifugation at 8000 *g* for 10 min, and dried under nitrogen. The residue was dissolved in 100 μl of methanol and analysed by HPLC on a reversed-phase C_{18} column. The sample was eluted with 100 % methanol at 25 °C at a flow rate of 1 ml/min. Absorbance of the eluent was monitored at 284 nm. Amounts of vitamin E or vitamin E succinate incorporated into cells were standardized based on the recovery of known amount of each compound added to the control cell suspension.

HPLC analysis of β-carotene in cells

The delivery of β-carotene was determined according to the method described by Offord et al. [27]. β-Carotene (10 mM) was dissolved in THF (tetrahydrofuran) and was added to a final concentration of 10 μM to DMEM containing 10 % FBS and 0.01 % Tween 20. After sonication for 1 min, the medium was sterilized by passing through an Acrodisc syringe filter with a 0.2 μm pore-size HT Tuffryn membrane (Pall, Ann Arbor, MI, U.S.A.). The cells (1×10^7) treated for 16 h with DMEM containing β-carotene were washed with PBS and lysed with 600 μl of lysis buffer (150 mM NaCl, 2 mM EDTA, 1 % Tween 20 and 100 mM Tris/HCl, pH 8.0). The cells were scraped and sonicated for 30 s in 15 ml plastic tubes, then mixed thoroughly with 0.8 ml of water, 1.6 ml of ethanol and 8 μl of deferoxamine mesylate (10 mg/ml) in the dark. The samples were extracted twice with 3.6 ml of n-hexane containing 0.03 % (w/v) BHT. After centrifugation for 5 min at 2000 *g* at room temperature (25 °C), the two supernatants were mixed and dried under nitrogen. The residue was dissolved in 100 μl of THF containing 0.03 % BHT and analysed by HPLC on a reversed-phase C_{18} column. The sample was eluted with 100 % methanol at 40 °C at a flow rate of 2 ml/min. The eluent was monitored by absorbance at 450 nm. The amount of β-carotene incorporated into cells was standardized based on the recovery of a known amount of each compound added to the control cell lysate.

Establishment of selenium-deficient cells

In order to establish selenium-deficient HepG2 cells, the serum concentration of the medium was decreased stepwise from 10 % to 1 % over 7 days as described previously [28]. Cells were used for experiments at least 7 days after being maintained in medium containing 1 % FBS. For the replenishment of selenium, sodium selenite (Wako, Osaka, Japan) was added to a concentration of 1 μM.

Measurement of total glutathione content in cells

Depletion of glutathione in HepG2 cells was achieved by treatment with 5 mM BSO (L-buthionine sulphoximine) (Sigma) for 24 h. Total glutathione was measured by the method described by Anderson [29]. Briefly, cells (1×10^6) were washed twice with PBS and suspended in 100 μl of 5 % sulphosalicylic acid by vigorous vortex-mixing. After centrifugation at 8000 *g* for 10 min, the supernatant was recovered for assay. Samples (10 μl) were mixed with the 980 μl of reaction mixture containing 100 mM sodium phosphate, pH 7.4, 5 mM EDTA, 0.6 mM 5,5′-dithiobis(2-nitrobenzoic acid) (Wako) and 0.3 mM NADPH. The increase in absorbance at 412 nm was monitored after the addition of 3 units of glutathione reductase (Roche, Mannheim, Germany). Authentic glutathione (Roche) solutions were used as a standard.

Enzyme assays

After washing once with PBS, cells were scraped from a culture dish and were collected by centrifugation at 500 *g* for 4 min. Cells were suspended in an appropriate volume of 10 mM Tris/HCl, pH 7.4, and were disrupted by a Bioruptor at 200 W for 30 s with cooling in ice-cold water. The supernatant was collected after centrifugation at 15000 *g* for 15 min, and was used in the assay of enzyme activities. SOD (superoxide dismutase) activity was

determined as described previously [30] using WST-1 [2-(4-iodophenyl)-3-(4-nitrophenyl)-5-(2,4-disulphophenyl)-2*H*-tetrazolium] (Wako) for the detection of generated superoxide anion. Briefly, the reaction mixture contained an appropriate amount of diluted xanthine oxidase (Roche), 0.1 mM xanthine (Wako), 0.025 mM WST-1, 0.1 mM EDTA, 50 mM $NaHCO_3$, pH 10.2, in a total volume of 3 ml. The increase in the absorbance at 438 nm was monitored at 25 °C for 1 min. One unit was defined as the amount of enzyme required to inhibit 50 % of the absorbance change of 0.060/min. This unit of enzyme activity is equivalent to that determined by the standard procedure using Nitro Blue Tetrazolium. CuZnSOD and MnSOD activities were defined as 2 mM NaCN-inhibitable activity and -resistant activity respectively.

GPx (glutathione peroxidase) activity was determined as described previously [30]. One unit was defined as the amount of enzyme required to oxidize 1 μmol of NADPH, corresponding to 2 μmol of GSH.

Caspase activity was determined essentially as described by Stennicke and Salvesen [31]. Acetyl-Leu-Glu-His-Asp-4-MCA (methyl-coumaryl-7-amide) and acetyl-Asp-Glu-Val-Asp-4-MCA were used for the measurement of caspase 9 and caspase 3 activity respectively. The reaction mixture contained 25 mM Pipes/KOH, pH 7.2, 5 mM $MgCl_2$, 10 mM DTT (dithiothreitol), 0.1 % CHAPS, 10 % sucrose and 0.05 mM substrate in a 200 μl volume. The initial rates of enzymatic hydrolysis were measured by the release of MCA from the substrate as the emission at 460 nm upon excitation at 380 nm using a BioLumin 960 Fluorometer (Molecular Dynamics, Tokyo, Japan) equipped with a thermostatically controlled plate reader.

Evaluation of the viability of cells by LDH (lactate dehydrogenase) activity

LDH activity was measured to assess the sensitivity of the cells to singlet oxygen [30]. At 24 h after treatment of cells in 24-well plates, portions of the medium were collected for measurement of LDH activity. The cells were collected and disrupted by brief sonication in PBS containing 0.1 % Tween 20. Cellular extracts free of debris were prepared by centrifugation at 15000 *g* for 10 min. The assay for LDH activity was performed using an LDH CII kit (Wako). The viability of the cells was calculated as the percentage of the LDH activity recovered in the cellular extract against the total (cellar extract plus medium) recovered activity.

SDS/PAGE and immunoblot analysis

Protein samples were subjected to SDS/PAGE with appropriate concentrations of polyacrylamide and then transferred on to a Hybond-P membrane (Amersham Biosciences, Little Chalfont, Bucks., U.K.) under semi-dry conditions by means of a Transfer-blot SD Semi-dry transfer cell (Bio-Rad). The membrane was then blocked by incubation with 5 % (w/v) skimmed milk in TBS (Tris-buffered saline; 137 mM NaCl, 2.7 mM KCl and 25 mM Tris/HCl, pH 7.6) containing 0.1 % Tween 20 for 2 h at room temperature. The membranes were then incubated with a mouse anti-(cytochrome *c*) Ig (1:1000 dilution) (Pharmingen, San Diego, CA, U.S.A.), rabbit anti-(caspase 3) IgG (H-277, Santa Cruz Biotechnology, Santa Cruz, CA, U.S.A.), rabbit anti-(human caspase 9) Ig (Cell Signaling Technology, Beverly, MA, U.S.A.), or rabbit anti-PARP IgG (H-250, Santa Cruz Biotechnology) for 16 h at 4 °C. After washing with TBS containing 0.1 % Tween 20, the membrane was incubated with 1:1000 diluted peroxidase-conjugated goat anti-mouse IgG or goat anti-rabbit IgG (Santa Cruz Biotechnology) for 1 h at room temperature. After washing, the peroxidase activity on the membranes was detected by a chemiluminescence method using an ECL® (enhanced chemiluminescence) Plus kit (Amersham Biosciences) and exposed to X-ray films (Kodak, Rochester, NY, U.S.A.). The amounts of protein were quantified by densitometric scanning of X-ray films using an Atto Densitograph (Atto, Tokyo, Japan).

Measurement of cytochrome *c* release from mitochondria in cells

Control cells or glutathione-depleted cells by incubation in 5 mM BSO-containing medium for 24 h were treated with endoperoxides or a precursor for 2 h, then incubated for an additional 4 h in fresh medium. Cytosolic fractions were prepared as described previously [32]. Briefly, 1×10^7 cells were scraped and washed in PBS, and suspended in 500 μl of a lysis buffer (250 mM sucrose, 50 mM Pipes/KOH, pH 7.4, 50 mM KCl, 5 mM EGTA, 2 mM $MgCl_2$, 1 mM DTT and 1 mM PMSF). After 30 min on ice, the cells were lysed with 40 strokes using pestle B in a Dounce homogenizer. After centrifugation at 14000 *g* for 15 min, the supernatant was regarded as the cytosolic fraction. Cytosolic proteins (10 μg) were subjected to immunoblot analysis.

Effects on cytochrome *c* release from isolated mitochondria

Mitochondria were isolated from rat livers by conventional subcellular fractionation. Briefly, 6 g of rat liver was homogenized in 3 vol. of solution A (0.32 M sucrose, 3 mM $MgCl_2$ and 20 mM Tris/HCl, pH 7.6), and the homogenate was filtered through cheesecloth. The homogenate was gently poured on to 20 ml of solution A in a 50 ml centrifuge tube, and centrifuged at 800 *g* for 10 min. The supernatant was centrifuged further at 8000 *g* for 10 min. The precipitate was suspended gently in 4 ml of a buffer (0.25 M sucrose, 1 mM $MgCl_2$ and 10 mM Tris/HCl, pH 7.6) by means of Dounce homogenizer using pestle B. All of the above procedures were performed at 4 °C. The isolated mitochondria were treated with each endoperoxide for 60 min followed by centrifugation at 12000 *g* for 10 min. Equal volumes of supernatants, containing approx. 20 μg of proteins, were separated and analysed as above.

Quantification of fragmented nuclei using fluorescence microscopy

After treated with MNPE or etoposide, cells were trypsinized, washed in PBS and suspended into PBS. Approx. 5×10^5 cells in 10 μl were stained with 0.03 mM DAPI (4,6-diamidino-2-phenylindole), and photographs were taken with a digital camera using a fluorescence microscope (Olympus BX 50, Tokyo, Japan). At least 500 cells on photographs were counted for calculating the percentages of the cells that had an intact, condensed or fragmented nucleus.

Detection of fragmented DNA by agarose gel electrophoresis

DNA was isolated from RBL-S1 cells (1×10^6 cells) according to the methods described by Ishizawa et al. [33]. Isolated DNA samples were electrophoresed on a 2 % agarose gel in Tris/borate/EDTA buffer. DNA was visualized on a UV illuminator after staining with 0.5 μg/ml ethidium bromide.

Evaluation of caspase activation in a cell-free system

Caspase activation in a cell-free system was achieved essentially according to a method described previously [34]. Briefly, HepG2 cell lysate was prepared in 4 vol. of buffer containing 0.32 M sucrose, 3 mM $MgCl_2$, 20 mM Tris/HCl, pH 7.5, 2 μg/ml aprotinin, 2 μg/ml pepstatin A, 50 μM (*p*-amidinophenyl)methanesulphonyl fluoride hydrochloride by homogenizing the cells with